Available online at www.sciencedirect.com
SCIENCE DIRECT®
International Journal of Heat and Mass Transfer 47 (2004) 2891–2900
International Journal of HEAT and MASS TRANSFER
www.elsevier.com/locate/ijhmt

Bubble-top jet flow on microwires

H. Wang [a], X.F. Peng [a,*], W.K. Lin [b], C. Pan [b], B.X. Wang [a]

[a] Department of Thermal Engineering, Tsinghua University, Beijing 100084, China
[b] Department of Engineering and System Science, Tsinghua University, Chinzhu 300, China

Received 17 November 2003; received in revised form 29 March 2004

Abstract

Bubble-top jet flows were investigated using high-speed photography and laser PIV (particle image velocimetry) technology. The bubble-top jet flow formation process was experimentally observed and described in detail. Pre-jet flows were also observed in advance of the jet flow formation in the early stage of bubble growth. The developed jet flow structure was divided into four different regions. In the pumped region, the hot liquid was pumped up from wire surface. The pumping effect was an important behavior of the jet flow, which caused highly efficient single-phase heat transfer near the bubble bottom, and also caused strong interactions between neighboring bubbles. The interaction and self-organization among the jet flows produced a relatively regular flow field. Bubble size greatly influenced the jet flow intensity and increased the complexity of the jet flow structure. Multi-jet flows were observed on larger bubbles. The experimental results suggest that the jet flows were induced by surface tension gradients or strong thermal non-equilibrium around a bubble rather than the evaporation and condensation within the bubble.

Keywords: Subcooled boiling; Bubble; Jet flow; PIV; Visualization

1. Introduction

Nucleate boiling is frequently encountered in a variety of practical applications, such as energy utilization, manufacturing systems and chemical engineering systems. In the last 50 years, a large number of studies were devoted to developing different correlations for predicting nucleate boiling heat transfer. However, no comprehensive theoretical models are yet available to accurately predict the heat and mass transfer of boiling processes [1,2].

Various heat transfer mechanisms have been proposed to explain the high heat transfer efficiency in nucleate boiling, such as bubbling (piston-like mechanism) [3], microlayer evaporation [4] in saturated boiling, and evaporation–condensation and quasi-cavitation in subcooled boiling [5]. With new developments in technology and the urgent need to more accurately predict heat transfer performance, boiling in unconventional environments has been increasingly investigated, especially for microscale and microgravity conditions. Many unusual dynamic processes were observed. Legendre et al. [6] presented a comprehensive numerical simulation of a single moving bubble. Lin [7] and Lin et al. [8] observed microscale homogeneous nucleation. Peng et al. [9,10] discussed the effect of spatial size on bubble formation. Glod et al. [11] investigated the explosive vaporization of water close to its superheat limit at microscale level using an ultrathin Pt wire. Nucleation jet and bubble sweeping on ultrathin wires were investigated in a sequence of experiments conducted by the authors' group [12–14]. These phenomena and their associated transport processes were considered as important complements to nucleate boiling heat transfer research. The impact of reduced gravity on pool boiling and bubble dynamics was investigated in the work of Rusanov and Shcherbakova [15] and Christopher et al. [16]. Boiling on downward facing inclined surfaces was also described [17–20].

* Corresponding author. Tel.: +86-10-6278-9751; fax: +86-10-6277-0209.
E-mail address: pxf-dte@mail.tsinghua.edu.cn (X.F. Peng).

0017-9310/$ - see front matter © 2004 Elsevier Ltd. All rights reserved.
doi:10.1016/j.ijheatmasstransfer.2004.03.023

Nomenclature

D_w	heater wire diameter (m)
q''_w	wire surface heat flux (W/m^2)
t	elapsed time (s)
T_b	bulk liquid temperature (K)
T_w	average wire temperature (K)
v	velocity (m/s)

Greek symbol

α	angle

Subscripts

b	bulk liquid
l	liquid
v	vapor
w	wire

Bubble-top jet flows, when liquid emanates from the bubble top into the bulk liquid to form a tail, is an interesting phenomenon first observed in downward-facing subcooled boiling [18–20]. Understanding of the jet flow phenomenon will help to improve available boiling heat transfer models, particularly the understanding of the competition between the microlayer evaporation and the heat removal by the liquid phase, both widely recognized as important mechanisms in boiling heat transfer. Various investigations made attempts to provide more experimental and theoretical evidences to better understand the physical nature of bubble-top jet flows [18–20]. The interfacial mass flux due to evaporation and condensation, the Marangoni effect induced by the surface tension gradient, and the surface pressure gradient resulting from evaporation [20] were supposed to make significant contribution to jet flows. However, the significance of these mechanisms is a topic of debate among different investigators. A more detailed systematic investigation is highly necessary to identify the phenomena and provide insight into their physical nature.

The present investigation includes a series of experiments conducted to further observe boiling phenomena, specifically jet flows for subcooled liquid boiling on ultrathin platinum wires. The structure and intensity of jet flows were visually and quantitatively measured and described. This experimental information was then used to analyze the various dynamic aspects of jet flows.

2. Experimental description

The experimental facility for high-speed photography experiments employed in the present investigation included three parts, the test section, the power supply and the high-speed photographic system, as shown in Fig. 1. The test section was a transparent vessel with a platinum heating wire placed in the vessel. The wire was installed horizontally or inclined at various angles. The platinum wires used in the experiments were 49 mm long and had diameter of 0.1 or 0.025 mm. The photographic system included a high-speed CCD camera, a high-resolution image acquisition card, and zoom lenses. The high speed CCD camera was a Kodak SR-Ultra digital video camera (Motion Corder Analyzer SR series) with a capability of up to 10,000 frames per second at resolution of 34×128 pixels. The sensor array of the camera was 658×496 pixels. The pixel size is 7.4 μm × 7.4 μm. The present experiments used recording rates of 500, 1000 and 2000 fps. The resolution was 512×480 pixels for speed less than 500 fps. The power supply provided direct current to the platinum wire generating Joule heat as the applied heat flux. The ends of the wires were connected to copper posts.

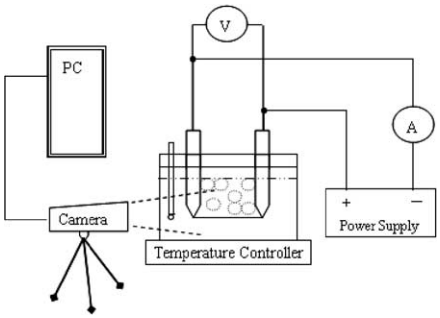

Fig. 1. Experimental setup.

The current and voltage to the platinum wire were measured to determine the input power and the wire resistance. The average wire temperature was then estimated using a calibrated correlation between the wire resistance and temperature. The resistance of the wire was approximately a linear function of the temperature and the temperature coefficient of resistance was calibrated as 3.85×10^{-3}/K. Before each experiment, the initial resistance of the Pt wire was determined at room temperatures. The change in resistance was then recorded during a test run with the temperature deduced from the calibration curve. An error analysis showed the overall uncertainty of the wire temperature measurement was ±3 K.

The pressure in the vessel was kept at atmospheric pressure. The bulk liquid temperature was measured using a thermocouple and a thermometer placed at the

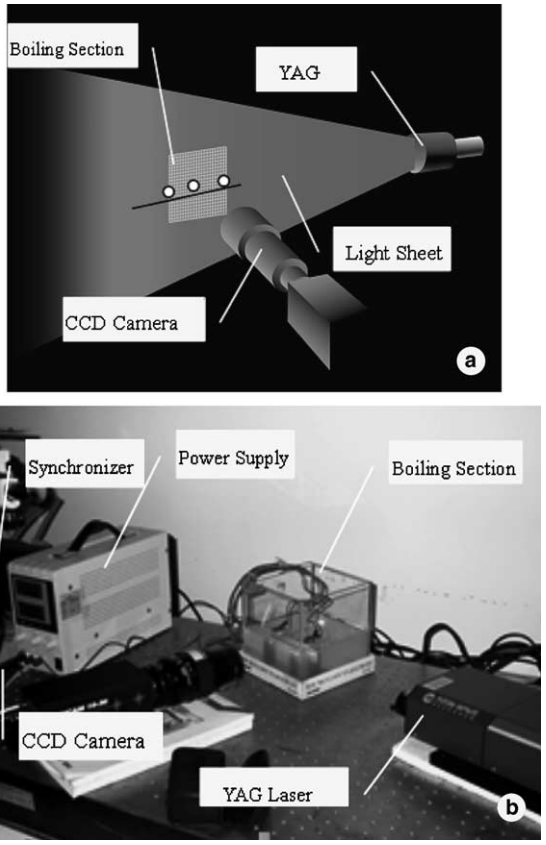

Fig. 2. PIV system. (a) PIV system for boiling test; (b) PIV system equipment.

different positions, 4 and 8 cm away from the wire, respectively. The measured bulk temperatures from the thermocouple and the thermometer agreed with each other within 2 K. The bulk temperature ranged from 293 to 373 K and the wire temperature ranged from 373 to 420 K for water boiling on a 0.1 mm wire with heat fluxes below 1.3×10^6 W/m^2.

2-D particle image velocimetry (PIV) technique was employed to measure velocity of flows. It provides the simultaneous visualization of streamline pattern in unsteady flows and the quantification of the velocity filed. The flow is seeded by small scattering particles. The instantaneous flow field was evaluated from recording and analyzing the tracer images.

The PIV system consisted of three major parts. (A) Imaging Subsystem, including laser, beam delivery system, light optics, produced pulsed laser to illuminate a plane in the seeded flow. (B) Image Capture Subsystem, including CCD camera, camera Interface, Synchronizer-Master control unit, captured the particle images and record them into computer. (C) Analysis and Display Subsystem, including Particle Image Velocimetry Software, analyzing and displaying two-dimension vector fields from the particle images. PIV system and experimental facility employed are illustrated in Fig. 2.

Because the bubbles on the heater wire were very small (commonly below 0.5 mm in diameter), the CCD camera in the PIV system was added with a series of zoom lens and aluminum oxide particles having 1 μm in diameter were used as seeding particles. The relative uncertainty of the velocity measurements from the system (including particle seeding, image recording, film digitization and PIV analysis) was estimated to be less than 5%. The uncertainty from the scale calibration was 3%. The overall uncertainty was less than 6%.

3. Jet flows from static bubbles

3.1. Formation of a bubble-top jet flow

For subcooled boiling at moderate heat fluxes, bubbles generally remained attached to the microheating wire for some time. With proper illumination, which was achieved by adjusting the intensity and the incidence angle of the lighting, jet flows were clearly observed and recorded using CCD system.

As shown in Fig. 3(f), from the top of a bubble attached to the wire, a strong flow penetrated into the bulk liquid for a long distance of up to 15 times of the wire diameter. Such a strong flow from bubble top is a so-called bubble-top jet flow in this paper. Although a jet flow was observed emanating from bubble top, the bubble top surface was intact without breaking. The bubble-top jet flow continued as long as its bubble stably stayed on the wire, normally 1–5 s at a moderate heat flux. Instantaneous local temperate fluctuations or flow field distortion could not produce such stable flows. When the heat fluxes were very high or the bulk liquid was close to saturated, bubbles did not remain attached to the wire and the jet flows stopped. Normally for water boiling on a 0.1 mm wire at the atmosphere pressure, the jet flows were easily observed at a heat flux below 1.1×10^6 W/m^2 and bulk temperature below 70 °C. For alcohol at same conditions, the jet flows were easily observed at a heat flux below 5.5×10^5 W/m^2 and bulk temperature below 50 °C.

When a bubble formed on the wire, its bubble-top jet flow did not immediately come forth but a short time was required for the jet flow to form and grow up. The growth process of a bubble-top jet flow was divided into two successive stages. In the series pictures, shown in Fig. 3 and taken at 500 frames per second, the first stage was from Fig. 3(a) and (b), lasting about 0.046 s. This is the preparation phase for the jet flow. The bubble first appeared in the frame shown in Fig. 3(a) (diameter about 0.05 mm) and stayed on the wire. At almost the same time, a weak flow pattern emerged around the bubble. The flow pattern did not change until $t = 0.046$ s

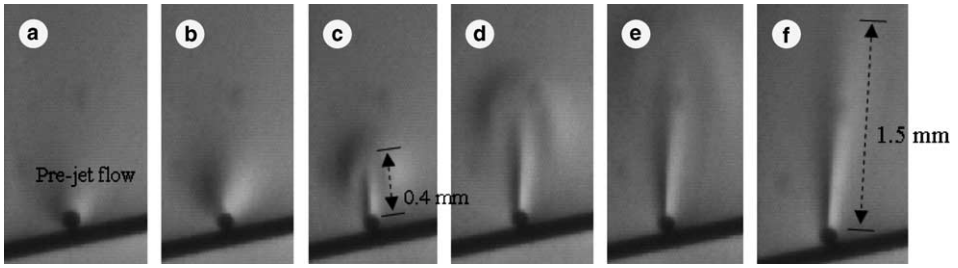

Fig. 3. Jet flow formation (water; $D_w = 0.1$ mm, wire $q''_w = 5.3 \times 10^5$ W/m^2, $T_w = 376$ K; $T_b = 330$ K). (a) $t = 0$ s, (b) $t = 0.046$ s, (c) $t = 0.058$ s, (d) $t = 0.076$ s, (e) $t = 0.098$ s, (f) $t = 0.138$ s.

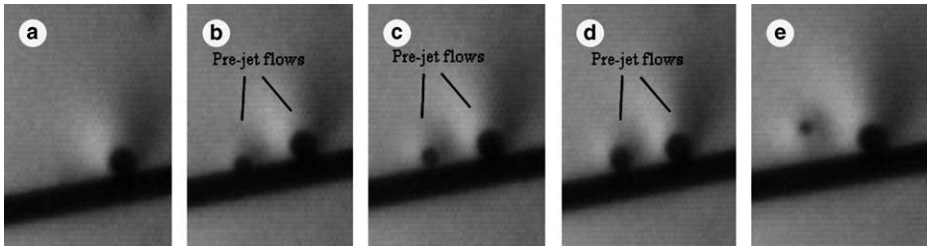

Fig. 4. Growing bubble with pre-jet flow (water; $D_w = 0.1$ mm, $q''_w = 6.0 \times 10^5$ W/m^2, $T_w = 377$ K; $T_b = 329$ K). (a) $t = 0$ s, (b) $t = 0.010$ s, (c) $t = 0.018$ s, (d) $t = 0.020$ s, (e) $t = 0.022$ s.

when the jet flow suddenly began to grow, as shown in Fig. 3(b). The flow pattern around the bubble in Fig. 3(a) did not behave like a jet flow but seemed to provide a preparation time for jet flow formation. The initial flow is termed as ''pre-jet flow'' here. Pre-jet flows formed very quickly (can be effectively observed within 0.01 s after bubble formation) and kept for a relative long time (0.046 s in Fig. 3). The pre-jet flow also appeared at very early stage in the bubble growth. Fig. 4 illustrates a growing bubble with its pre-jet flow (the stable bubble on the right side of the growing bubble also had a pre-jet flow). The dynamic characteristics of early stage of bubble growth, including bottom temperature fluctuations, are rationally supposed to be highly associated with the pre-jet flow.

The second stage of the jet flow growth is shown in Fig. 3(b)–(f), during which the jet flow developed and penetrated into the bulk liquid. An arc shaped shock-type wave formed at the front edge of the jet flow, which grew up as it moved away from the bubble. The wave front velocity was estimated to be 34 mm/s in Fig. 3(c). Finally, the wave front disappeared as the jet flow achieved its fully developed form, as shown in Fig. 3(f). The second phase took about 0.92 s.

One of interesting phenomena observed is that some bubbles did not always remain attached to the wire. A few of little bubbles first jumped into the bulk fluid, then returned to the wire surface and finally produced jet flows, as shown in Fig. 5. After the jet formed, the bubble remained attached to the wire. The Marangoni

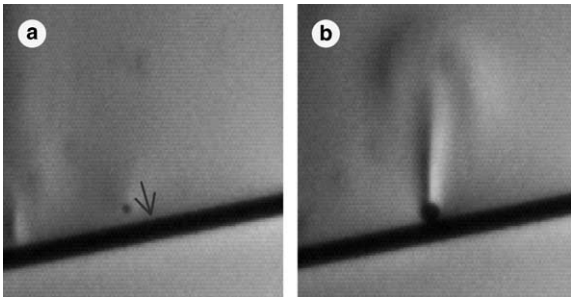

Fig. 5. Bubble re-attached to the wire. (a) Bubble re-attaching; (b) Jet flow.

flow around the bubble was expected to exert a force on the bubble that prevents the bubble from detaching [21]. Both attached bubbles and detached bubbles would be pushed towards the wire by the Marangoni force as long as they were in a temperature gradient region [22]. The bubble re-attaching should imply the importance of Marangoni flow in these experiments.

3.2. Jet flow structure

The streamline around the bubbles was traced with a small quantity of floc particles (diameter about 10 μm and specified weight approximately equal to 1.0) added into the bulk water. The properties of the bulk water would not be altered by the particles since the particle

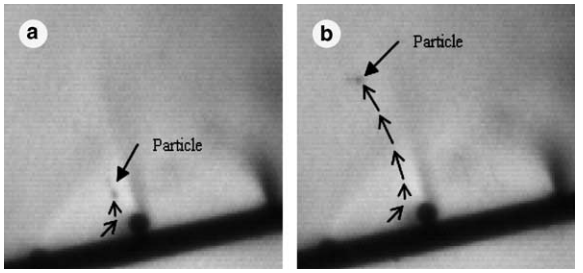

Fig. 6. Suspended particle tracing jet flow (water; $D_w = 0.1$ mm, $q''_w = 6.0 \times 10^5$ W/m^2, $T_w = 379$ K; $T_w = 325$ K).

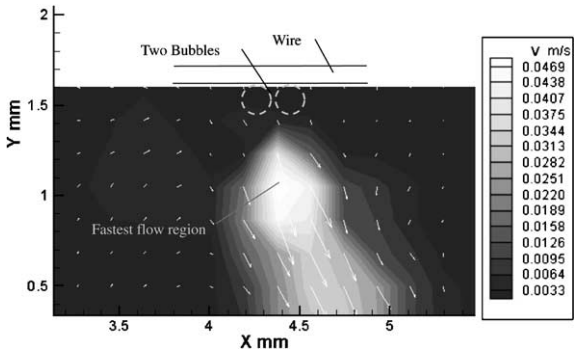

Fig. 8. Velocity vector and contours (m/s) (water; $D_w = 0.1$ mm, $q''_w = 5.8 \times 10^5$ W/m^2, $T_w = 379$ K; $T_b = 310$ K).

concentration was very small, normally below 15 particles/mm^3. Fig. 6 illustrates the track of a particle dragged by the jet flow. A particle, in Fig. 6, initially on the left side of the bubble, was sucked towards the bubble by the jet flow. The floc particle moved up along the side of the bubble and was then ejected into the bulk liquid together with the jet flow. The particle track clearly illustrated the jet flow configuration. The particle velocities were 57 mm/s in Fig. 6(a) and 37 mm/s in Fig. 6(b), indicating that the jet flow decelerated as it moved away from the bubble.

More detailed information was obtained from the PIV measurements shown in Figs. 7 and 8. In Fig. 7(a) the arrows represent the local velocity vectors with the arrow length representing the relative velocity magnitude. Fig. 7(b) shows the velocity contours of the jet flow in Fig. 7(a). The fastest flow was 35 mm/s, having same magnitude measured by the CCD system.

From Fig. 7(b), the fastest flow was not at the bubble top surface, but some distance (about 0.8 mm) away from the bubble. In Fig. 8, two downward facing bubbles produced a coalesced jet flow that flowed downward with the fastest flow region about 0.3 mm away from the bubbles. These fastest flow regions verify that the bubble-top jet flow was not induced by the mass flux induced by condensation or vaporization on the bubble top surface. If the mass flux at the bubble top played a major role in forming the jet flow, the fastest velocities ought to be exactly at the bubble top.

Typically, a developed bubble-top jet flow could be divided into four regions, pumped region, jet neck, expanding and wake region, as shown in Fig. 9. The pumped region is around the bubble bottom where the hot liquid around the wire is pumped up along the bubble surface and concentrated to form a strong jet flow at the jet neck. The pumped region strongly influences the heat transfer around the bubble. The jet flow begins to expand in the expanding region above the neck and fluid density in this region still differs from that in surrounding bulk liquid. The top end of the jet is the wake region where the flow is disappearing and merges with the bulk liquid. There is no distinct boundary

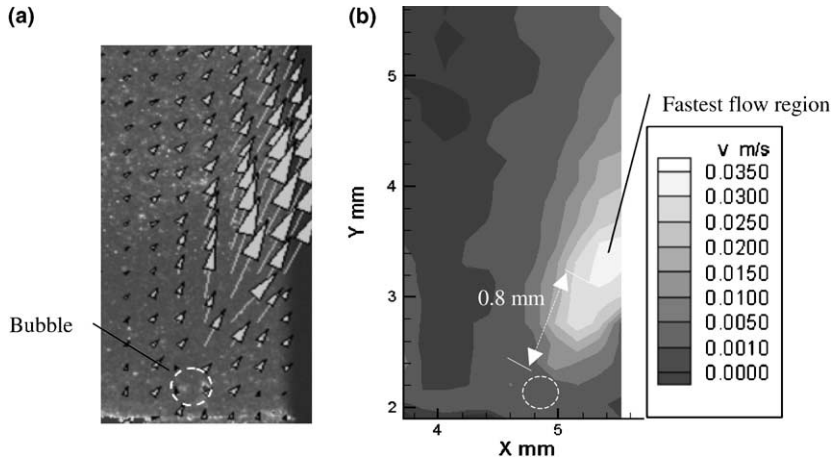

Fig. 7. Jet flow measured by PIV system (water; $D_w = 0.1$ mm, $q''_w = 5.9 \times 10^5$ W/m^2, $T_w = 382$ K; $T_b = 320$ K). (a) Velocity vector; (b) velocity contours (m/s).

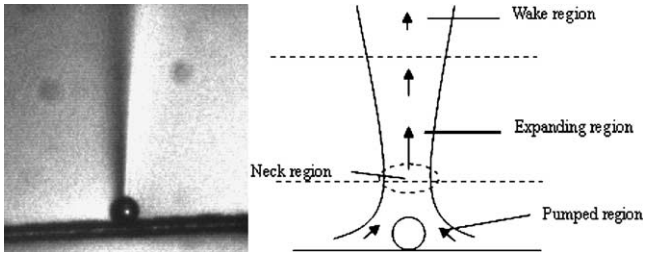

Fig. 9. Bubble-top jet flow structure.

between the jet flow and the bulk liquid, not like a bubble having its interface.

3.3. Jet flow intensity and driving forces

Jet flow intensity is an important parameter that can be related to the physical mechanisms driving the flow around the bubble. Normally, in experiments of subcooled water on a 0.1 mm platinum wire, the measured velocities ranged from 10 to 140 mm/s. For examples, the wave front moved upward at 34 mm/s in Fig. 3(c), in Fig. 6 the tracing particle velocity reaching to 57 mm/s, and in Figs. 7 and 8 the fastest flow velocities were 35 and 49 mm/s, respectively.

Jet flow intensity was strongly dependent upon bubble size. Smaller bubbles usually had stronger jet flows than larger bubbles, as shown by the CCD images, Fig. 10(a), and the PIV measurements, Fig. 10(b). Previous investigations [19] presumed that the condensation at the bubble top played an important role in forming jet flows. If so, a jet flow from a larger bubble ought to be more intensive because the top of a larger bubble stretches farther into the colder bulk liquid than with a smaller bubble. In addition, in Fig. 10(b), the flow between the two large bubbles I and II was stronger than the flow at their top, which indicates that the jet flow was not from the bubble top but from the lower surface and moved up around the bubble. The downward jet flows in Figs. 8 and 10 also exclude natural convection as a driving force for the jet flows. As noted in previous investigations [21,22], Marangoni flow should be considered as an important factor causing the jet flows.

4. Dynamic behavior of jet flows

4.1. Competition and self-organization of jet flows

The pumping effect of each jet flow greatly influenced the flow field and the temperature distribution nearby. If two jet flows were close to each other, their pumped regions overlapped and interactions occurred. In the experiments, strong interactions were frequently observed between neighboring jet flows. The competition restrained some bubble-top jet flows, or caused others to coalesce into a stronger flow when they were close enough. Fig. 8 shows a coalesced jet flow from two close bubbles. Inside a group of bubbles on the wire, the jet flows from different bubbles usually coalesced into a stronger, larger and more stable jet flow, as shown in Fig. 11, here termed "jet column". A jet column commonly included three to five or more individual jet flows. The competition between the jet columns was similar to that observed between the individual jet flows as they competed for the pumped liquid. A weak jet column often formed near a strong jet column as shown in Fig. 11. The self-organization among the columns finally produced a regular and relatively steady flow field in the boiling system.

In addition to the bubble-top jet flows, there is another kind of strong flow observed during boiling on

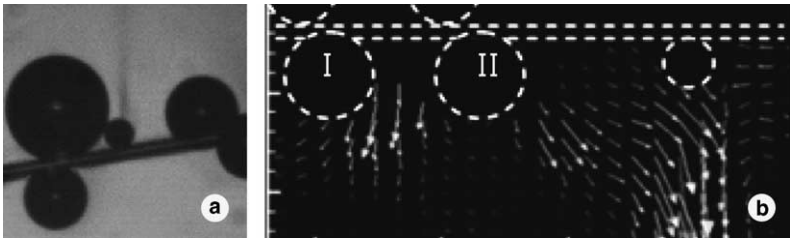

Fig. 10. Effect of bubble size on jet flow. (a) CCD image; (b) PIV measurements.

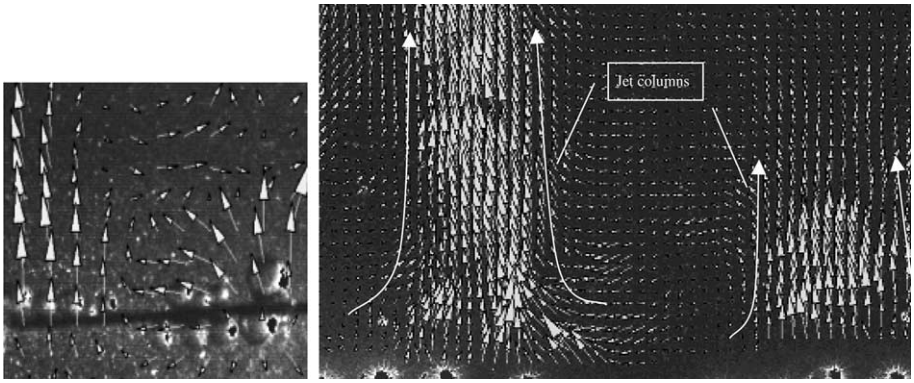

Fig. 11. Bubble jet flow columns.

microwires, nucleation jet flow [12]. Such jet flows were vapor–liquid mixtures ejected directly from nucleation sites without a normal bubble growth process. Fig. 12 illustrates how a bubble-top jet flow attracted a nucleation jet flow. The darker color of the nucleation jets relative to the bubble top jet flows shows that the density of the nucleation jets might be much less than that of the bubble-top jets. In Fig. 12(a) the nucleation jet was

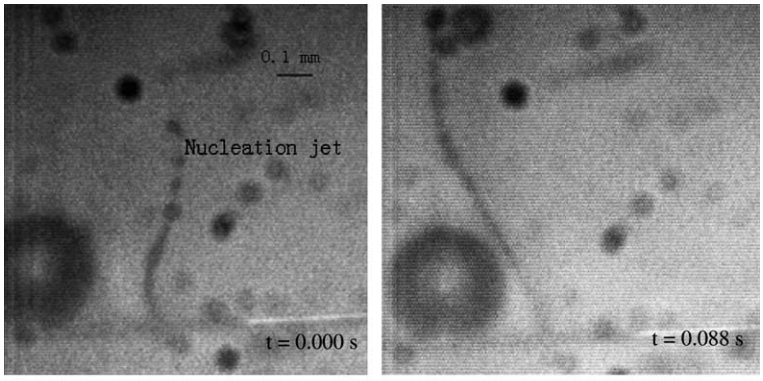

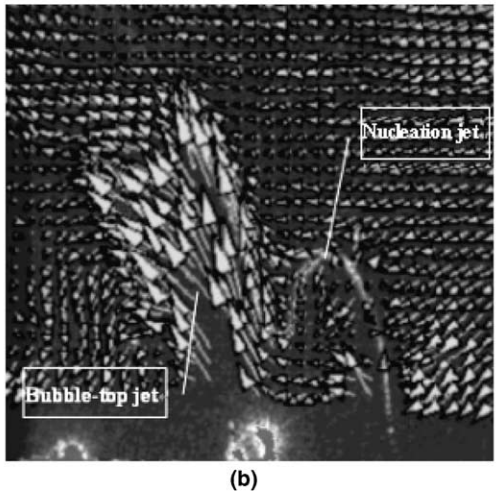

Fig. 12. Interaction between a bubble-top jet and a nucleation jet. (a) CCD observations (95% alcohol; $D_w = 0.025$ mm, $q''_w = 1.8 \times 10^6$ W/m^2, $T_w = 470$ K; $T_b = 310$ K). (b) PIV measurement (water; $D_w = 0.1$ mm, $q''_w = 5.8 \times 10^5$ W/m^2, $T_w = 382$ K; $T_b = 315$ K).

initially ejected upward, but its direction was soon changed towards the bubble. Fig. 12(b) shows a flow field measured by the PIV system including a bubble-top jet and a nucleation jet. The nucleation jet was greatly distorted by the bubble-top jet as it was drawn towards the bubble.

4.2. Jet flows from moving bubbles

Vapor bubbles were occasionally observed automatically moving back and forth along the wires in the experiments as shown in Fig. 13. Moving bubbles reversed their directions when they encountered with other bubbles on the wire. Usually a moving bubble did not stop until it grew large enough to depart. When a bubble started to move, its bubble-top jet flow could still be observed, as shown in Fig. 13(b) [13,14], like a tail following the bubble. The mechanism driving the moving bubbles is rarely understood. PIV measurements were then used to gain further experimental information for getting insight into the nature, as shown in Fig. 14. Very clearly, the jet flow is almost vertical. The jet flows applied only a downward thrust to keep the bubbles attached to the wire, while without any forces to push the bubbles moving horizontally.

The pumping effect of the jet flows was more obvious during bubble moving. In Fig. 15, before the bubble moved through, a hot liquid layer can be seen attached

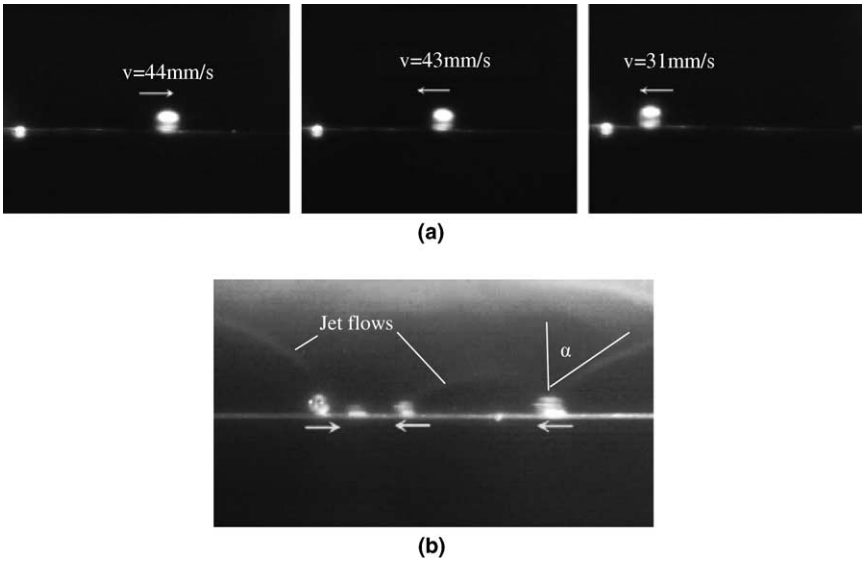

Fig. 13. Moving bubbles and their jet flows [13]. (a) Bubble moving back and forth along the wire; (b) moving bubbles with their jet flows.

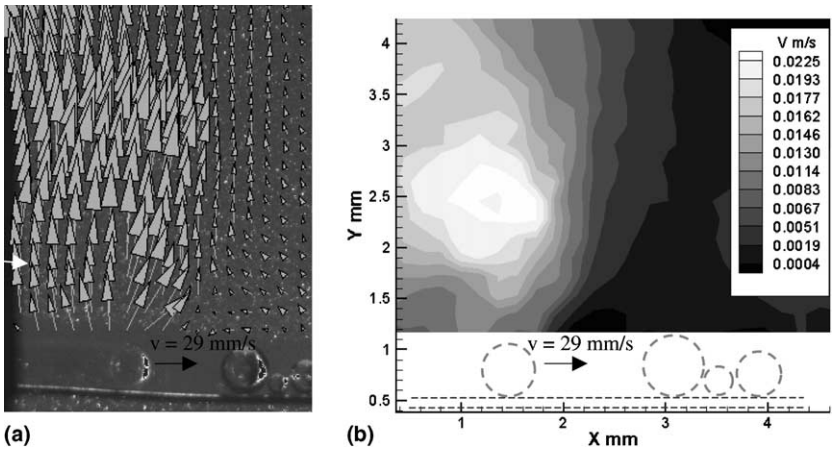

Fig. 14. Moving bubble jet flow measured by PIV. (a) Velocity vector; (b) velocity contours.

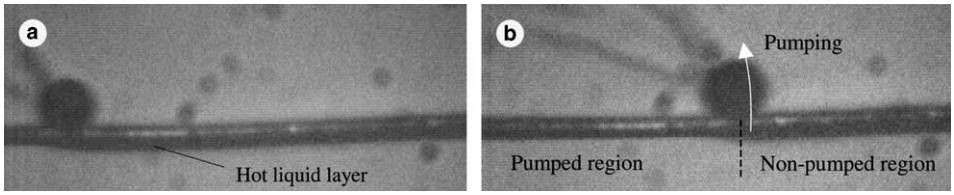

Fig. 15. Pumping effect of a moving jet flow. (a) $t = 0$ s; (b) $t = 0.022$ s.

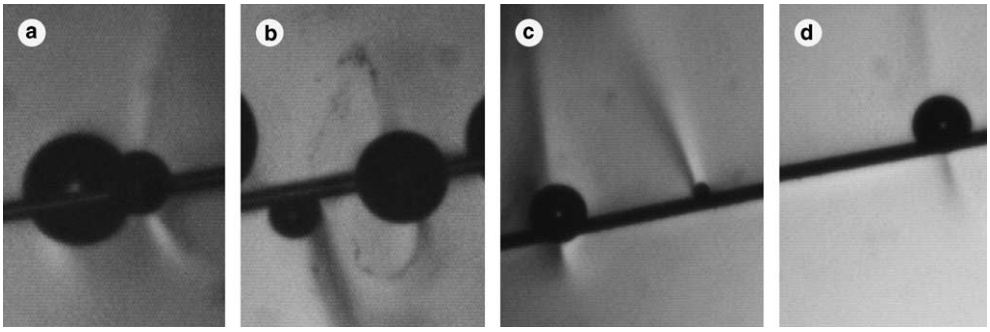

Fig. 16. Multi- jet flows.

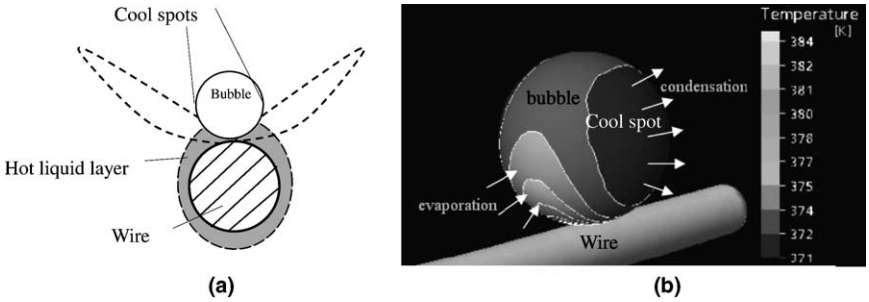

Fig. 17. Temperature distribution on bubble surface with multi-jet flows. (a) Multi-bubble jet flow; (b) Temperature on a larger bubble.

to the wire, and after the bubble moved through, the thick hot liquid layer was reduced to a thinner hot liquid layer, as the two regions illustrated. This is the consequence of the pumping effect of the bubble. Previous observations of bubble sliding phenomena [23,24] did not discuss the pumping effects of a bubble.

4.3. Multi-jet phenomenon

As shown in Fig. 16, one bubble on the wire might have two jet flows from its two sides. The experimental observations showed that smaller bubbles had only a single bubble-top jet flow while larger bubbles tended to have more than one jet flow, as seen in Fig. 16(c). In previous experiments conducted on downward-facing plates, each bubble had only a single jet flow [18–20]. The size of a bubble relative to the heating wire is thought to be an important factor for multi-jet flow structure. Small bubbles are almost completely immersed in the hot liquid layer around the wire. As a result, the bubble surface temperature uniformly decreases from the bottom to top. For larger bubbles, however, not only their tops, but also their two sides stretch into the cooler liquid. Two cold spots exist on the two sides of the bubbles, as illustrated in Fig. 17, and may simultaneously induce two jet flows from the two sides. Further experimental observation is highly necessary to understand multi-jet phenomenon.

5. Conclusions

High-speed photography and laser PIV (particle image velocimetry) technology were employed to

experimentally observe and investigate the flow structure around bubbles during subcooled boiling on ultrathin platinum wires. Various types of jet flow structures were observed and described.

The bubble-top jet flow formation process began with a pre-jet flow having a relatively small flow region near the bubble. The jet flows and pre-jet flow ought to be general phenomena existing in subcooled liquid boiling, which means strong thermodynamic non-equilibrium.

The developed jet flow structure was observed and exhibited four regions, pumped region, neck region, expanding region and wake region. In the pumped region, hot liquid is pumped up from the bottom of the bubble into the bulk liquid. The pumping effect is important mechanism in jet flows causing considerable single-phase heat transfer from the heating wire and around the bubble, and also strong interactions among neighboring bubbles. The interactions and self-organization among individual jet flows created a stronger jet flow in the subcooled boiling system. Moving bubble jet flow and multi-jet flow were also observed, and these phenomena are highly dependent upon the pumping effect induced by strong thermal non-equilibrium around bubbles.

Acknowledgements

This work was supported by the National Natural Science Foundation of China (Contract nos. 59625612 and 59976016).

References

[1] V.K. Dhir, Nucleate and transition boiling heat transfer under pool boiling and external flow conditions, in: Proc. 9th Int. Heat Transfer Conf., Jeruslem, Israel, vol. 1, 1990, pp. 129–155.

[2] V.P. Carey, Liquid Vapor Phase-transition Phenomena, Hemisphere Publishing House, New York, 1992.

[3] M. Jacob, Heat Transfer, vol. l, Wiley, New York, 1949, pp. 614–657.

[4] F.D. Moore, R.B. Mesler, The measurement of rapid surface temperature fluctuations during nucleate boiling of water, AIChE J. 7 (4) (1961) 620–624.

[5] Y.I. Nesis, I.S. Sologub, Temperature fluctuations in subcooled boiling at a single site, in: Kipenie i Kondensatsia, RPI Press, Riga, 1984, pp. 5–13.

[6] D. Legendre, J. Boree, J. Magnaudet, Thermal and dynamic evolution of a spherical bubble moving steadily in a superheated or subcooled liquid, Phys. Fluids 10 (6) (1998) 1256–1265.

[7] L.W. Lin, Microscale thermal bubble formation–thermal physical phenomena and applications, Microscale Thermophys. Eng. 2 (2) (1998) 71–82.

[8] L.W. Lin, A.P. Pisano, V.P. Carey, Thermal bubble formation on polysilicon micro resistors, J. Heat Transfer 120 (3) (1998) 735–746.

[9] X.F. Peng, H.Y. Hu, B.X. Wang, Boiling nucleation during liquid flow in microchannels, Int. J. Heat Mass Transfer 41 (1) (1998) 101–110.

[10] X.F. Peng, H.Y. Hu, B.X. Wang, Bubble formation of liquid boiling in microchannels, Sci. China Ser. E: Technol. Sci. 41 (4) (1998) 404–411.

[11] S. Glod, D. Poulikakos, Z. Zhao, G. Yadigaroglu, An investigation of microscale explosive vaporization of water on an ultrathin Pt wire, Int. J. Heat Mass Transfer 45 (2) (2002) 367–379.

[12] H. Wang, X.F. Peng, B.X. Wang, D.J. Lee, Jet flow phenomena during nucleate boiling, Int. J. Heat Mass Transfer 45 (6) (2002) 1359–1363.

[13] H. Wang, X.F. Peng, B.X. Wang, D.J. Lee, Bubble sweeping and jet flows during nucleate boiling of subcooled liquids, Int. J. Heat Mass Transfer 46 (5) (2003) 863–869.

[14] H. Wang, X.F. Peng, B.X. Wang, D.J. Lee, Bubble-sweeping mechanisms, Sci. China Ser. E 46 (3) (2003) 225–233.

[15] K.V. Rusanov, N.S. Shcherbakova, Effect of reduced gravity and weightlessness on vapor bubble dynamics and heat transfer in boiling liquid, Low Temp. Phys. 24 (2) (1998) 100–115.

[16] D.M. Christopher, B.X. Wang, X.F. Peng, Flow field around a condensing and evaporating vapor bubble in microgravity, in: Proc. Molecular and Microscale Heat Transfer in Material Processing and Other Applications, Part 2, 1996, pp. 162–170.

[17] G.F. Naterer, W. Hendradjit, K.J. Ahn, J.E.S. Venart, Near-wall microlayer evaporation analysis and experimental study of nucleate pool boiling on inclined surfaces, J. Heat Transfer 120 (3) (1998) 641–653.

[18] I.G. Shekriladze, On the role of the Pumping Effect of a vapor bubble growing at the wall during nucleate boiling, in: Voprosy konvektivnogo teploobmena I chistoty vodianogo para, Metsniereba Press, Tbilisi, 1970, pp. 90–97 (in Russian).

[19] X.F. Peng, Y.J. Huang, D.J. Lee, Transport phenomenon of a vapor bubble attached to a downward surface, Int. J. Therm. Sci. 40 (9) (2001) 797–803.

[20] I.G. Shekriladze, Sh.A. Mestvirishvili, J.G. Rusishvili, G.I. Zhoszholiani, V.G. Ratiani, Studies in the mechanism of boiling and of enhancement of evaporative cooling coefficients, Heat Transfer-Sov. Res. 12 (2) (1980) 91–95.

[21] R. Marek, J. Straub, The origin of thermocapillary convection in subcooled nucleate pool boiling, Int. J. Heat Mass Transfer 44 (3) (2001) 619–632.

[22] N.O. Young, J.S. Goldstein, M.J. Block, The motion of bubbles in a vertical temperature gradient, J. Fluid Mech. 6 (1959) 350–360.

[23] K. Cornwell, I.A. Grant, Heat transfer to bubbles under horizontal tubes, Int. J. Heat Mass Transfer 41 (10) (1998) 1189–1197.

[24] G.E. Thorncroft, J.F. Klausner, R. Mei, An experimental investigation of bubble growth and detachment in vertical upflow and downflow boiling, Int. J. Heat Mass Transfer 41 (23) (1998) 3857–3871.